



ELSEVIER

Biochimica et Biophysica Acta 1369 (1998) 267–277

[View metadata, citation and similar papers at core.ac.uk](#)

brought to you by CORE

provided by Elsevier - Publisher Connector

# Peptide–liposome association. A critical examination with mastoparan-X

Nadja Hellmann <sup>\*,1</sup>, Gerhard Schwarz*Department of Biophysical Chemistry, Biocenter of the University of Basel, Klingelbergstr. 70, Basel, Switzerland*

Received 10 June 1997; revised 18 September 1997; accepted 19 September 1997

## Abstract

Mastoparan-X, a wasp venom factor, is a membrane active peptide whose binding to lipid vesicles is of basic interest towards an analysis of its functions. Titration of aqueous peptide solutions with liposomes allows the determination of the association isotherm, i.e. a plot of bound peptide per lipid versus the free peptide concentration. We have scrutinised the various steps in the evaluation procedure, considering circular dichroism as well as fluorescence intensity as possible signals for the binding process. First of all the measured data had to be corrected for light scattering effects which may otherwise appreciably falsify the final results. Uncertainties due to inherent difficulties regarding the reproducibility of lipid preparations and inevitable titration errors have to be considered. The consequences of these errors for the quantitative analysis of the titration curves were investigated. The plotted curves can be reasonably well fitted by a functional relationship derived from a Gouy–Chapman model approach that assumes a partitioning of monomeric peptide. The two relevant parameters, partition coefficient and effective charge number, and their error ranges have been determined for mastoparan-X and a series of phosphatidylcholine vesicle sizes and various ionic strengths. These findings show that the applied analysis implies a sufficient basis for calculations of the amount of lipid bound peptide in practice. However, the possible existence of peptide aggregates cannot generally be excluded from a formal monomer associated curve fit as indicated by computer simulations. © 1998 Elsevier Science B.V.

**Keywords:** Peptide–lipid interaction; Partition equilibrium; Light scattering correction; Salt effect; Error source; Peptide aggregation

## 1. Introduction

The wasp venom peptides of the mastoparan family (including mastoparan-X) are toxic tetradecapep-

tides that have attracted much attention because of their diverse biologically significant activities on membranes. They cause degranulation of mast cells [1–3], stimulate the enzymatic catalysis of phospholipase A<sub>2</sub> [4] and also activate G-protein functions as they mimic a G-protein receptor [5,6]. Thus it is of basic interest to investigate their binding affinity to lipid membranes. In our laboratory we have especially been concerned with the mastoparan-induced pore formation in lipid vesicles [7,8]. In that case reliable data on the extent of peptide association with liposomes were badly needed. From the technical

Abbreviations: POPC, palmitoyllecithin; DOPC, dioleoylphosphatidylcholine; NBD-PE, *N*-(7-nitrobenz-2-oxa-1,3-diazol-4-yl)-1,2-dihexadecanoyl-*sn*-glycero-3-phosphoethanolamine, triethylammonium salt

\* Corresponding author. Fax: +49 6131 393 557; E-mail: nadja@biologie.biophysik.uni-mainz.de

<sup>1</sup> Present address: Institute for Molecular Biophysics, Jakob-Welder-Weg 27, University of Mainz, 55128 Mainz, Germany.

point of view it appeared quite appropriate to point out major requirements of a dependable data processing routine. In particular, we refer to the present examination of light scattering effects that affect the quality of final results but have not been considered so far. Therefore our study provides a more generally applicable line of procedures in the field of peptide(protein)–liposome binding systems.

In this study the binding curves were determined both by circular dichroism and fluorescence spectroscopy, reflecting the conformational change of the peptide upon binding [9,10]. The influence of lipid species (DOPC,POPC), NaCl-concentration and the size of vesicles was investigated. Effects of light scattering on these measurements and the propagation of titration errors in the course of data evaluation from the original titration curves to the final isotherms were quantified. This allows an assessment of the reliance in the experimentally obtained model-free binding isotherm.

The theoretical description of the binding process is based on a partitioning equilibrium of the peptide between two phases: the aqueous and the lipid-phase [11,12]. The interaction between the peptides on the membrane has usually to be taken into account in terms of an appropriate activity coefficient. The activity coefficient for electrostatic interactions can be derived from the Gouy–Chapman model for the diffuse double layer [13]. This approach yields in the case of partitioning of monomers two parameters: the difference in the chemical standard potential of free and bound peptide, expressed by a partition coefficient  $K_p$ , and the effective charge of the peptide,  $z_{\text{eff}}$ . The usefulness of this simple approach will be discussed and an extension that includes possible aggregation in the membrane will be given.

## 2. Materials and methods

### 2.1. Chemicals

All experiments were carried out with synthetic mastoparan-X (Bachem Feinchemikalien, Bubendorf, Switzerland). Small amounts of concentrated stock solutions of the peptide ( $\approx 300 \mu\text{M}$ ) in buffer were stored at  $-20^\circ\text{C}$ . Stock solutions were usually thawed only once to minimise peptide degradation. The con-

centration of the stock solution was determined photometrically using an absorption coefficient  $\epsilon = 5600 \text{ cm}^{-1} \text{ mol}^{-1}$  for the tryptophan residue.

Lipids (POPC,DOPC) were purchased from Avanti Polar Lipids (Birmingham, Alabama, USA), dissolved in chloroform. NBD-PE was from Molecular Probes (Eugen, Oregon, USA). Long-time storage of lipids was done in chloroform at  $-20^\circ\text{C}$ . Dried lipid films were stored under argon and used within a week.

The buffer solution contained 10 mM Hepes (Bio-probe, France), 1 mM EDTA (Merck, Darmstadt, Germany) and various concentrations of sodium chloride (Merck). The pH was adjusted to 7.4 if not mentioned otherwise.

### 2.2. Vesicle preparation

Lipids in chloroform were pre-dried in a glass tube by rotary evaporation and dried overnight under oil-pump vacuum. The lipid film was dissolved in buffer solution and vortexed shortly. For sonified vesicles this solution was treated with a tip-sonifier (MSE, London, Great Britain) for 50 min. After sonification the solution was centrifuged for 10 min at 10 000 rpm on a Eppendorf table-centrifuge to remove titanium debris splintered from the tip. The size distribution was checked by dynamic light-scattering [14]: about 93% of the particles were distributed around a diameter of  $12 \pm 1 \text{ nm}$  with a half-width of 3 nm. About 7% of the vesicles had a size of 50 nm. For the preparation of extruded vesicles the lipid-solution was subjected to 5 freeze-thaw-cycles in liquid nitrogen. The solution was extruded 5 times through a coarser filter and 5 times to the filter of chosen size (filter from Costar, Cambridge, MA, USA). Using a filter of 50 nm diameter, the size distribution had a maximum at 70 nm diameter with a half-width of 10 nm (S.Rex, personal communication). The use of filters with pores of 100 nm diameter yielded vesicles distributed around 100 nm with a similar half-width. The lipid concentration of the vesicle stock solution was between 5 and 20 mM. The exact concentration in the solution was determined by phosphate analysis [15]. Especially the size distribution of the sonified vesicles showed a detectable scattering for different vesicle preparations due to a restricted reproducibility of the relevant physical properties. The vesicles were

used for experiments within a few hours after preparation.

### 2.3. Fluorescence measurements

The experiments were performed on a spectrofluorometer F777 (Jasco, Tokyo, Japan), equipped with one monochromator in each light path. The excitation wavelength was set at 280 nm (1.5 nm bandwidth) and the emission wavelength at 320 nm (3 nm bandwidth). Quartz cells (Hellma, Müllheim, Germany) with a path length of 0.4 cm were used in order to reduce volume, absorption and scattering artifacts. Solutions were filtered through a 0.45  $\mu\text{m}$  filter to remove dust. Mixing of added volumes in the titration experiments was performed by gentle turnover of the sealed cuvette. The solutions were carefully thermostated at 20°C. No time dependence of the signal could be detected after 1 min. The peptide concentration at the beginning of each titration experiment was determined via the fluorescence signal in absence of vesicles.

### 2.4. Circular dichroism

Measurements were performed on a CARY 61 (Cary, Monrovia, CA, USA). In order to optimise the signal/noise ratio, the path length of the quartz-cuvettes (Hellma, Müllheim, Germany) was varied depending on the peptide concentration (2 mm–10 mm). Solutions were filtered through a 0.45  $\mu\text{m}$  filter. All measurements were done at a fixed wavelength of 220 nm. Baseline stability was checked at 260 nm, where none of the components gave a contribution to the signal. The bandwidth was adjusted automatically corresponding to the signal to noise ratio. The signal was accumulated until the deviation from the average was less than 5% per added measured value. Any effect on the signal resulting from absorption is corrected automatically in the recording procedure.

### 2.5. Theoretical basis

The principles of data evaluation of association measurements have recently been reviewed [12]. The main points are to be briefly summarised here, so that

we can examine any consequences of possible lipid associated peptide aggregation. The association isotherm is determined by a defined functional relationship between the concentration of bound and free peptide. This function might be implicitly defined, but is unambiguously depending on the thermodynamic properties characterising the system. These are the partition coefficient  $K_p$  (partitioning of the peptide monomer between aqueous and lipid phase), several equilibrium constants  $K_i$  describing the stepwise aggregation of  $i$  monomers within the lipid membrane and appropriate activity coefficients  $\alpha_i$ . As pointed out in [11] the partitioning of charged monomers can be described by a simple mass action law combined with an activity coefficient for electrostatic interaction:

$$r = K_p c_f / \alpha \quad \alpha = \exp(2 z_{\text{eff}} \sinh^{-1}(z_{\text{eff}} b r)) \quad (1)$$

The free peptide concentration is denoted  $c_f$ , whereas  $r = c_{\text{as}}/c_L$  is the bound (“associated”) peptide per lipid. The parameter  $b$  is a constant depending on temperature and ionic strength. In order to consider also aggregation in the membrane we add appropriate mass action equations to the monomer partitioning:

$$r_1 = K_p c_f / \alpha_1, \quad \alpha_i r_i = K_i \alpha_{i-1} r_{i-1} \alpha_1 r_1$$

(where  $r_i = c_i/c_L$ ,  $i = 2, 3, \dots$ ) (2)

The total amount of bound peptide is  $r = \sum_{i=1}^n i r_i$ , where  $r_i$  is the concentration of peptide in units of oligomers and  $r$  in units of monomers. For the activity coefficients of oligomers different effective charges per monomer,  $z_i$ , may be introduced. Then we obtain

$$\alpha_i = \exp(2 i z_i \sinh^{-1}(b x)) \quad x = \sum_{i=1}^n i z_i r_i \quad (3)$$

Allowances for different effective charges for different aggregation levels are made because of the approximative character of the Gouy–Chapman-model when applied to a functional expression of the activity-coefficients. Generally substantial deviations between effective charge number and the physical charge has been observed. These might depend on the detailed topology of the bound peptide [16,17]. A main drawback of the inclusion of different effective charges is, that now the association isotherm is not a

simple function of merely the two experimentally available quantities  $r$  and  $c_f$ : formally  $r$  is replaced by the quantity  $x$  which is connected with  $r$  via numerous unknowns, namely the  $z_i$  and  $r_i$ .

## 2.6. Data evaluation

The binding isotherm can be obtained in a model independent way from the data. A typical experiment is started with a solution of a given peptide concentration to which aliquots of lipid-stock solution are gradually added. An appropriate measuring signal  $\Phi$  (depending linearly to different extents on free and bound peptide) is employed to monitor the binding process. The value in absence of vesicles is denoted by  $\Phi_0$ .

After correcting for the contribution of lipids a normalised signal  $F$  is defined according to

$$F := (\Phi - \Phi_0)/c_P = F_\infty r c_L / c_P$$

$$F_\infty := \sum_{i=1}^n (F_i - F_f) r_i / r \quad (4)$$

Here  $F_f$  is the specific signal of free peptide and  $F_i$  the signal of the  $i$ -meric peptide on the membrane. The total concentrations of peptide and lipid are  $c_P$  and  $c_L$ , respectively. In cases where the bound peptide exhibits an unique signal which does not depend on the aggregation level,  $F_\infty$  is constant over the total titration course and the quantity  $Q := F c_P / c_L$  is proportional to the bound peptide ratio  $r$ . If it is not known a priori, whether  $F_\infty$  will depend on  $r$  or not, one has to determine the change of  $F_\infty$  with  $r$ . This procedure is described in detail elsewhere [12,18–20]. A dependence of  $F_\infty$  on  $r$  indicates a change of signal upon aggregation on the membrane. However, a constant course can be caused either by lack of change in the value of  $F_i$  upon aggregation or by lack of aggregation at all.

## 3. Results

### 3.1. Correction of the data for scattering effects

#### 3.1.1. Fluorescence

The consequences of light scattering when doing fluorescence measurements were investigated, since even for small sonified vesicles a considerable frac-

tion of light is scattered under the experimental conditions applied here (e.g. 20% at 1 mM lipid, 1 cm path length, 280 nm).

It could be shown both from experiments and theoretical considerations, that the intensity of emitted light is not influenced by scattering due to the spatial isotropy of emission. This is true, if no polarisation has to be taken into account. The correction factor obtained by the following method is solely a consequence of scattering of the excitation light.

In order to distinguish between the changes of fluorescence intensity due to binding from scattering artifacts, we measured the liposome induced reduction of fluorescence of single tryptophan. We could show that tryptophan does not interact with lipid membranes. The observed reduction of fluorescence was related to the fraction of light scattered by vesicles ( $I_s/I_0 = x_s$ ), so that different vesicles sizes can be described with one correction factor. The fraction of scattered light is a linear function of the lipid concentration in the investigated concentration range. The fluorescence of single tryptophan decreases linearly with the fraction of scattered light and can be described with the following empirical relation up to the values of  $x_s = 0.3$ :

$$(\Phi - \Phi_{\text{lipid}}) / \Phi_0 = (1 - 0.65 x_s) := \gamma \quad (5)$$

Here  $\Phi$  is the fluorescence of tryptophan in presence,  $\Phi_0$  the fluorescence in absence of vesicles and  $\Phi_{\text{lipid}}$  the contribution of vesicles. The value for  $x_s$  can be determined with a simple photometer since the lipids do not absorb considerably at 280 nm. The data obtained in the titration experiments with mastoparan-X were corrected according to the relation

$$\Phi_{\text{corr}} = (\Phi_{\text{meas}} - \Phi_{\text{lipid}}) / \gamma \quad (6)$$

This corrected value was used for further data analysis. As the exact value of the correction factor 0.65 shown in Eq. (5) depends on the optical geometry of the apparatus and type of cuvettes, it has to be determined individually for a given experimental setup. The correction to be applied to sonified vesicles is less than 5% up to 1 mM lipid concentration when working with half-micro cuvettes.

#### 3.1.2. Circular dichroism

Although any effect of background absorption is eliminated due to the data recording, the effect of

scattering on the signal is still visible, probably due to depolarization of the light. The influence of the presence of vesicles could easily be measured by using a double-chamber cuvette. One chamber was filled with peptide solution to give the signal, the other was filled with solution of increasing concentration of lipid-vesicles. The signal from the solution containing only vesicles was subtracted. These experiments were done with cuvettes of different path-length. An empirical correction-factor depending on the vesicle concentration and the pathlength could be obtained from these measurements:

$$\theta_{\text{corr}} = \theta_{\text{meas}} \exp(2.410^{-4} d c_L)$$

Here  $\theta$  is the signal in [mdeg cm<sup>2</sup> /dmol] and  $d$  the length of the cuvette in [cm]. The lipid concentration  $c_L$  is given in [ $\mu\text{M}$ ]. This equation was obtained for sonified vesicles, which is the only size used for our CD-measurements.

### 3.2. MPX-binding to DOPC- and POPC-vesicles

The model-independent isotherms for the binding of mastoparan-X to POPC and DOPC vesicles were determined after correction for light scattering. For a quantitative analysis Eq. (1) was fitted to the data.

#### 3.2.1. Fluorescence measurements

No clear dependence of the value for  $F_\infty$  on the fraction of associated peptide could be found, irrespective of the amount of added salt. The average of  $F_\infty$  for each data set did not depend on vesicle size or concentration of added salt.

An example of a titration experiment (original data) and an association isotherm is given in Fig. 1(A) and (B). In this case two experiments under the same conditions were performed. In Fig. 1(A) the recorded data prior to any corrections are shown. Correction of the data for dilution and according to Eq. (6) yields the corresponding association isotherm from the procedure described in [12], which is displayed in Fig. 1(B). Here the hollow circles represent the original data and the full circles mean values: the values of the free peptide concentration corresponding to similar values of  $r$  were averaged. The error bars represent typical standard errors. Both curves (original and averaged) were fitted. The fitted curves are matching each other quite well, although the

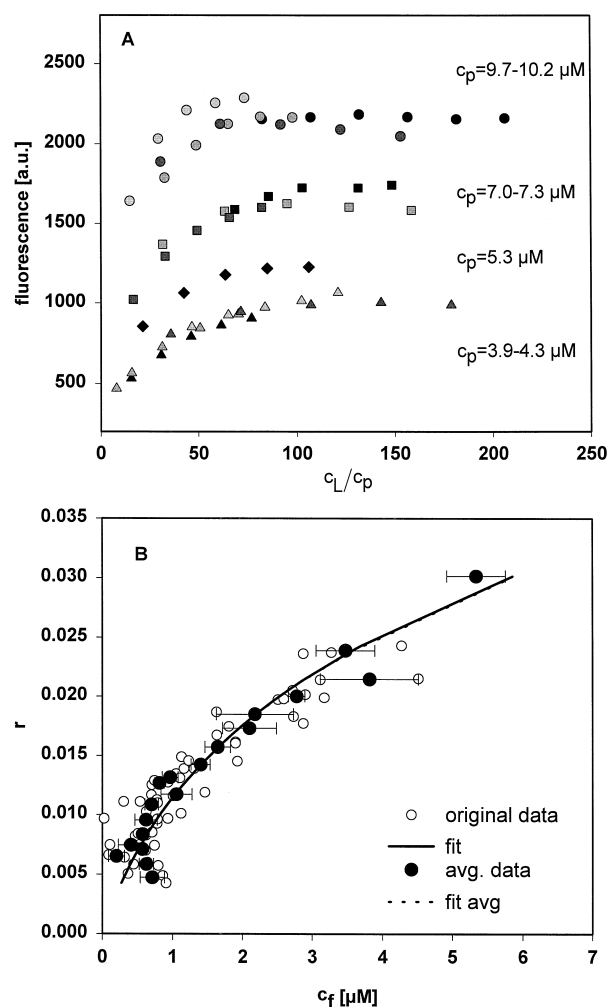


Fig. 1. Binding data for the association of mastoparan-X with DOPC sonified vesicles in presence of 400 mM NaCl. (A) Change in fluorescence of tryptophan in the sequence of mastoparan-X as a consequence of binding to vesicles. Data were obtained by titration of vesicles to solutions with different concentrations of the peptide (see legend). The data are obtained from two different vesicle preparations. Each set of symbols correspond to one titration experiment, where 5 or 6 aliquots of lipid solution were added to the peptide solution. Black symbols correspond to the lower limit, light grey to the higher limit of the concentration range given in the figure. (B) Model-free binding isotherm obtained by the procedure described in the text. The value for  $F_\infty$  was constant for the total titration course. An equation derived for the partitioning of monomers (Eq. (1)) was fitted to the data (hollow circles), yielding  $K_p = 1.9 \times 10^4 \text{ M}^{-1}$ ,  $z_{\text{eff}} = 2.1$ . Averaged data (full circles) were also fitted which gave  $K_p = 2.6 \times 10^4 \text{ M}^{-1}$ ,  $z_{\text{eff}} = 2.5$ . The values for the fitted parameters differ, although the calculated curves are very similar.

fitted parameters are not identical (see legend to Fig. 1). The errors for the fit parameters given by the fitting routine are typically 5% for  $z_{\text{eff}}$  and 10–15% for  $K_p$ . The actually observed deviations are larger due to the strong numerical dependence of the values of the two parameters on each other, which causes a strong dependence of the results on minor variations in the data. In the following comparisons only the averaged values of the data points are shown, in order to make the figures clearer.

The influence of ionic-strength was investigated in the range of 0 to 400 mM added NaCl for DOPC and POPC vesicles. In this range no aggregation of the peptide in solution occurs. Increasing the salt concentration leads to a stronger binding of the peptide to the membrane (Fig. 2(A)). The effect of salt is more pronounced in the case of DOPC than in the case of POPC. The increase in the amount of bound peptide is mainly the result of a reduced electrostatic repulsion, as reflected by the reduced value of  $b$ . The influence of size was investigated for POPC at 100 mM NaCl. Increasing the size of the vesicles leads to a reduced association (Fig. 2(B)). The results of fitting Eq. (1) to the data are shown in Table 1. For these results the original curves, not the average, were fitted. In case of POPC the fitted partition coefficient has a tendency to decrease with increasing ionic strength. However, the effective charge does not change monotonously. In case of DOPC the tendency is reversed for the partition coefficient, whereas the variation in the effective charge is similar. On average, the effective charge in case of DOPC is somewhat smaller than for POPC.

In order to enlarge the change in signal upon peptide-binding also measurements with 0.3% NBD-PE incorporated as an acceptor of energy-transfer of the tryptophan fluorescence were performed (data not shown). Here no significant change in the isotherm compared to experiments without NBD-PE could be found: the small amount of NBD-PE did not alter the properties of the membrane. So this could be a useful alternative for peptides for which the increase of fluorescence intensity upon binding is less pronounced than for mastoparan-X. Experiments at different pH values, ranging from 7.0 to 8.5 did neither result in a significant change. Thus the pH is not a critical experimental parameter in this range (data not shown).

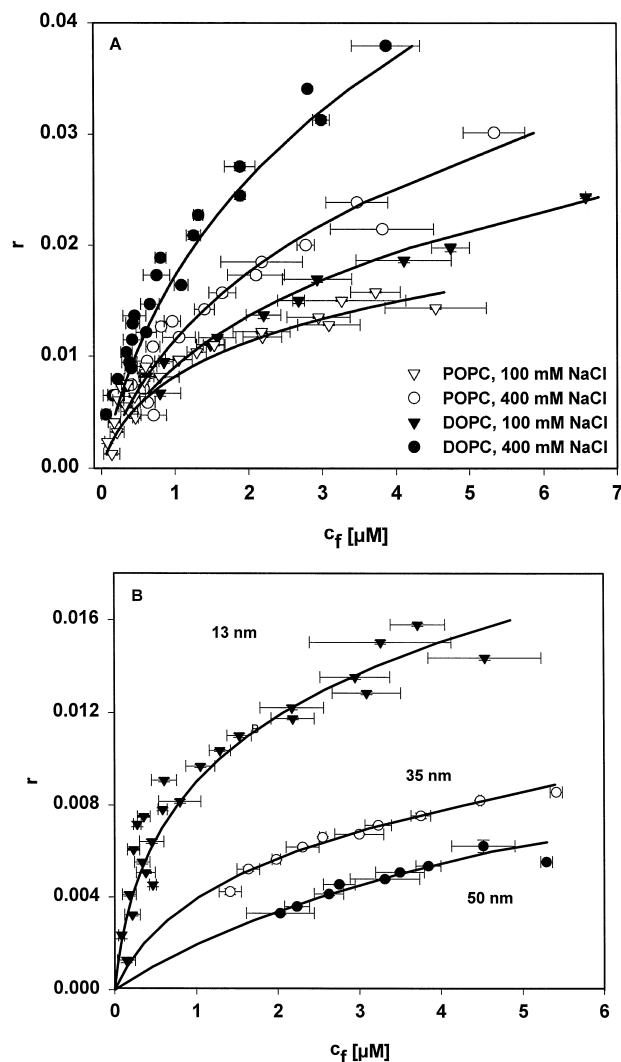


Fig. 2. Comparison of averaged binding isotherms for different systems obtained by fluorescence spectroscopy. (A) Influence of lipid-composition and concentration of NaCl. (B) Influence of the size for POPC vesicles, radius as given in the figure. The values for the fit-parameters are given in Table 1.

### 3.2.2. Circular dichroism

The correction of the CD-data lead to an increase in the value for  $F_{\infty}$ , which resulted in decreased values for  $K_p$  and  $z_{\text{eff}}$ . We refer to the example of POPC (at 100 mM NaCl) in Table 1, where the partition coefficient is subject to a drop by a factor of more than 3!. This has to be taken into account, when these results are compared to those published earlier [19]. Only with the presented correction the isotherm obtained from CD-measurements was actually consistent with the fluorometrically determined curve (see

Table 1  
Partition coefficient and effective charge

Fluorescence				
Radius	Lipid	NaCl [mM]	$K_p$	$z_{\text{eff}}$
13 nm	POPC	0	$3.6 \pm 0.9$	$1.9 \pm 0.1$
		100	$2.2 \pm 0.3$	$2.5 \pm 0.1$
		200	$1.8 \pm 0.3$	$2.3 \pm 0.1$
		400	$1.9 \pm 0.2$	$2.1 \pm 0.1$
13 nm	DOPC	0	$1.4 \pm 0.3$	$1.4 \pm 0.1$
		100	$1.6 \pm 0.2$	$1.8 \pm 0.1$
		200	$1.8 \pm 0.3$	$2.0 \pm 0.1$
		400	$3 \pm 0.4$	$1.8 \pm 0.1$
35 nm	POPC	100	$0.9 \pm 0.1$	$3.0 \pm 0.1$
50 nm	POPC	100	$0.4 \pm 0.07$	$2.4 \pm 0.6$

Circular dichroism, vesicle radius 13 nm				
Correction	Lipid	NaCl [mM]	$K_p$	$z_{\text{eff}}$
no	POPC	100	$7.6 \pm 2$	$2.6 \pm 0.2$
yes	POPC	100	$2.3 \pm 0.5$	$2.2 \pm 0.1$

Values of the fitted parameters of the association isotherm on basis of Eq. (1), yielding the partition coefficient  $K_p$  and the effective charge  $z_{\text{eff}}$  (the errors are those given by the fitting procedure). Values for different radii and salt concentrations are given. ‘Correction’ is meant with respect to light scattering effects. For the circular dichroism data we found  $F_\infty = 13.5 \text{ deg cm}^2 \text{ dmol}^{-1}$  for the uncorrected data, and  $F_\infty = 16.6 \text{ deg cm}^2 \text{ dmol}^{-1}$  for the corrected data. Here only sonified vesicles were investigated. The partition coefficient is given in  $K_p/10^4$ ,  $[K_p] = \text{M}^{-1}$ . The values for the parameter  $b$  (Eq. (1)) are: 23 (0 mM), 9.7 (100 mM), 7 (200 mM), 5 (400 mM).

Table 1). The difference between corrected and not corrected values in the CD-measurements is considerable even for sonified vesicles in contrast to fluorescence measurements, where it is less pronounced due to the lower wavelength employed for the CD-measurements.

## 4. Simulations

### 4.1. Influence of experimental uncertainties

In any experiment of the type mentioned here uncertainties in the concentrations are inevitable. As the data evaluation is quite complex, the propagation of errors is difficult to determine analytically. Therefore we addressed this problem by simulations. In a

minimal approach only errors in the lipid concentration were considered, since these accumulate in our experiments. Based on Eq. (1) isotherms for certain values of  $K_p$  and  $z_{\text{eff}}$  were calculated. The corresponding original data like shown in Fig. 1(A) were obtained by using typical values for the fluorescence signal of bound and free peptide and calculating the corresponding sum. In order to mimic titration errors, an error for the lipid concentration in the range between  $-3\%$  and  $+3\%$  was introduced randomly. When these ‘real’ curves were evaluated according to the standard routine, the intended, correct lipid concentration is employed like it is the case in a real experiment. With no errors included, the input parameters for  $K_p$  and  $z_{\text{eff}}$  were obtained from the data evaluation routine as it must be. For the data with titration errors three runs were done with new random numbers and otherwise identical parameters. The criteria for judging the influence of these errors on the results were stability of  $F_\infty$  and possible deviation of the fit-parameters  $K_p$  and  $z_{\text{eff}}$  from the input values.

The values of  $F_\infty$  in relation to the input value are shown in Fig. 3 for three simulations. Obviously, small titration errors could fake a monotonous change in  $F_\infty$  (see sim1, sim2 in Fig. 3). From this figure it must be concluded that the change in the value of  $F_\infty$  has to be larger than 20% to be significant. The fit of Eq. (1) to the corresponding isotherms yielded values for  $K_p$  and  $z_{\text{eff}}$  as shown in Table 2. Surprisingly, the fitted values of the partition coefficient can vary up to 25% compared to the true input value, although the simulated titration errors are very small. The effective charge is less affected. Since here only one error-source is included, the error in a real experiment will be larger.

The variations in the fit parameters are partly caused by the high interdependence of the two parameters  $K_p$  and  $z_{\text{eff}}$  when a fitting procedure is applied. This leads to a strong dependence of the fitting results on small variations in the data set. Connected with this problem is the dependence of the fitted parameters on the measured range of  $r$ . It could be shown that the fitted effective charge is the more reduced compared to the input value, the more the concentration range for the fit is restricted to regions, where the effective charge does not influence the amount of bound peptide very much. This should also

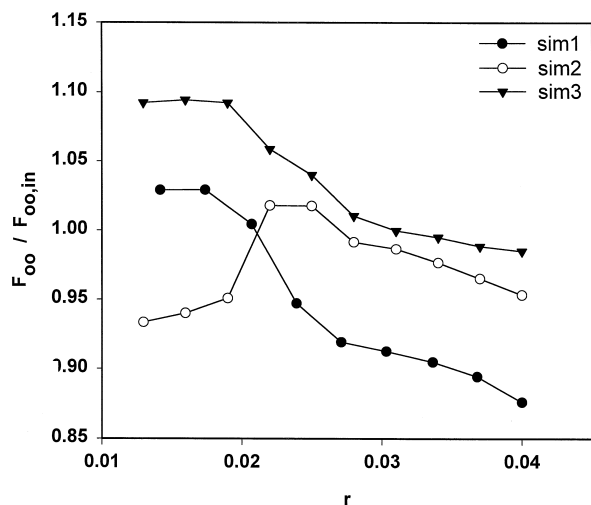


Fig. 3. Influence of titration errors on  $F_{\infty}$ . A typical experiment was simulated three times. For calculation of the ‘data’ all concentrations and measured values were assumed to be correct except the lipid concentration. The lipid concentration was varied randomly in the range of  $-3\%$  and  $+3\%$  around the correct values. For the data evaluation the correct value for the lipid concentration was used. For each simulation new random numbers were calculated, leading to three slightly different binding isotherms. The values determined for  $F_{\infty}$  as given in the text were plotted as ratio to the input value. Small titration errors can apparently fake a monotonous change in  $F_{\infty}$ . The results of fitting Eq. (1) to the corresponding binding isotherms (data not shown) are given in Table 2. The value for  $F_{\infty}$  given therein is the mean of those shown in Fig. 3.

be taken into account when fit parameters of different curves are compared.

The determination of  $F_{\infty}$  is of great importance. Fig. 4 shows how the fitted parameters depend on the value of  $F_{\infty}$ . The effect of an error of 4% in  $F_{\infty}$  can be quite dramatic concerning the value of  $K_p$ . The effective charge  $z_{\text{eff}}$  is far less affected. The error in  $F_{\infty}$  can indeed be significant especially when the

Table 2  
Fitted parameters for simulations

Curve	$K_p / 10^4 [\text{M}^{-1}]$	$z_{\text{eff}}$	$F_{\infty}$ (mean)
no error	$2.05 \pm 0.007$	$2.06 \pm 0.003$	$2.55 \pm 0.003$
sim. 1	$2.63 \pm 0.24$	$2.05 \pm 0.07$	$2.41 \pm 0.05$
sim. 2	$2.48 \pm 0.29$	$2.06 \pm 0.09$	$2.45 \pm 0.02$
sim. 3	$1.48 \pm 0.09$	$1.85 \pm 0.06$	$2.64 \pm 0.04$

The errors for  $K_p$  and  $z_{\text{eff}}$  are those given by the fitting routine; the errors for  $F_{\infty}$  are standard errors of the mean. Input parameters:  $K_p = 2 \cdot 10^4 \text{M}^{-1}$ ,  $z_{\text{eff}} = 2$ ,  $F_{\infty} = 2.55$ .

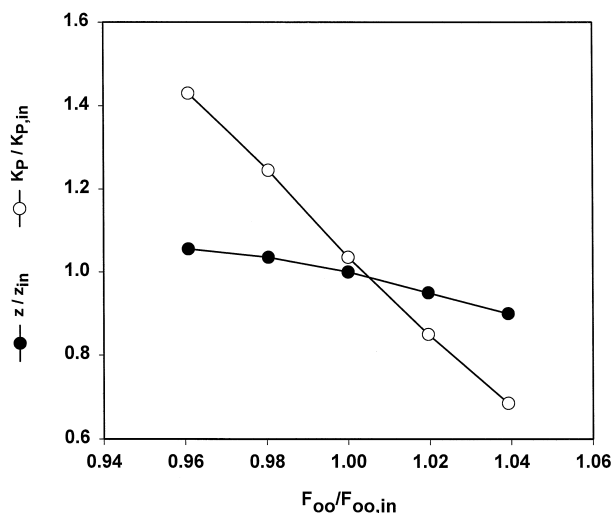


Fig. 4. Dependence of the fitted values of  $K_p$  and  $z_{\text{eff}}$  on  $F_{\infty}$ . An experiment was simulated, where all values are precisely determined except the value of  $F_{\infty}$ , for which an error of up to  $\pm 4\%$  was assumed. The corresponding binding isotherms were calculated and values for the partition coefficient and effective charge were determined. The ratio between these fitted values and the input values is plotted versus the relative error of  $F_{\infty}$ . An inaccurate determination of only 4% error can cause an error in the partition coefficient as large as 40%!

value of  $F_{\infty}$  is determined by extrapolation of the normalised signal  $F$  for  $c_L / c_P \rightarrow \infty$  as it is often done.

#### 4.2. Aggregation of peptide within the membrane

Another question to be raised is whether the approach used for obtaining the fit function (Eq. (1)) does represent the underlying processes. It is not evident, whether aggregation processes in the membrane always change the shape of the association isotherm compared to the monomeric case. Therefore we calculated isotherms for different sets of input parameters for Eqs. (2) and (3), including aggregation up to tetramers. All peptide molecules composing an oligomer had an identical value of the effective charge in our calculations. Only for the monomers a different effective charge was allowed. The isotherms were simulated in a concentration range ( $c_L, c_P$ ) which was similar to the range in our experimental data. In Fig. 5 an example for an isodesmic case ( $K_1 = K_2 = K_3 = K_4$ ) is shown, where the aggregation constant increases, whereas all other parameters remain con-



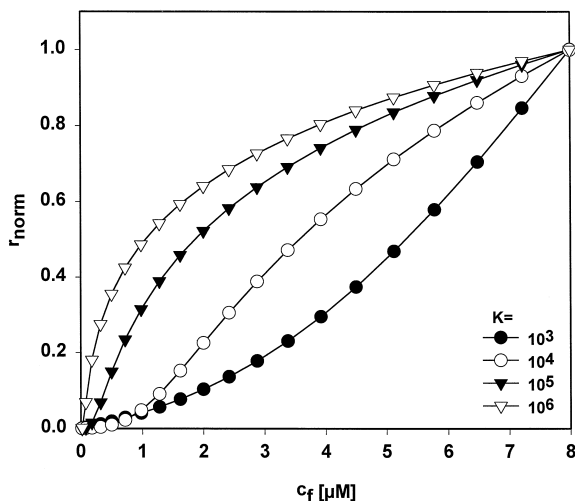


Fig. 5. Simulation of binding isotherms including aggregation on the membrane. This example shows an isodesmic case for aggregation on the membrane up to tetramers, e.g. the aggregation constant for each successive step is identical. For a comparison of the shape the data were normalised with respect to the value at  $8 \mu\text{M}$  of free peptide. The partition coefficient was  $100\text{M}^{-1}$  and the effective charge both for monomers and oligomers was 2. The aggregation constant  $K$  was varied between  $10^3$  and  $10^6$ . For a low aggregation constant the onset of aggregation within the membrane occurs at relatively high peptide concentration ( $K = 10^3, 10^4$ ). For a large aggregation constant practically all of the membrane-associated peptide is oligomerised, so that the shape of the isotherm is not distinguishable from one which reflects the partitioning of monomers ( $K = 10^6$ ).

stant. For a aggregation constant of  $K = 10^4$  the curve shows a critical concentration, where the aggregation process starts. The curve with  $K = 10^6$  would not be distinguishable from the case of a monomer partitioning. Apparently an isotherm involving a high degree of aggregation resembles an isotherm of pure monomers. This could be the reason why comparatively few examples of isotherms reflecting aggregation have been reported so far.

In the concentration range accessible by the methods used here we note that data are not very reliable below  $1 \mu\text{M}$  of free peptide. Thus all isotherms, which deviate only below this threshold from the monomeric behaviour, were fitted with a monomeric curve (data not shown). Some rules could be established with regard to the relation between input parameters and fitted values. The fitted effective charge is always smaller or equal to the maximum of the input values. A change in the partition coefficient or

aggregation constants leads to a change in the fitted effective charge even if the input effective charges are kept constant. The fitted value of  $z_{\text{eff}}$  changes towards the value of the oligomers when the aggregation constants increase. For the fitted partition coefficient not much can be said. Of course the fitted value is always greater or equal to the input partition-coefficient. There is no straightforward way of correlating the value for the fitted partition coefficient in Eq. (1) with the aggregation constants in Eq. (2). We infer from these simulations that unless one is sure that there is no aggregation on the membrane, the parameters fitted with a model for partitioning of monomers might not reflect significant thermodynamic parameters of the system but a kind of average of several unknowns. It is not possible to extract the aggregation constants by fitting Eq. (3) to the data directly due to the large number of parameters.

## 5. Discussion

Isotherms for the binding of mastoparan-X to DOPC and POPC vesicles of different sizes and under varying ionic strength were recorded. The aim of these investigations was to determine the amount of bound peptide and to analyse the thermodynamic parameters of this binding by applying an appropriate model.

Comparing the isotherms themselves, the results found for mastoparan-X are in line with results found for other membrane-active peptides like common mastoparan, which has a related sequence [19,21]. In both cases the degree of association increases with salt concentration. This is mainly caused by a reduction of the activity coefficient due to a lower value for  $b$  in Eq. (1). For mastoparan the salt-effect for POPC is more diminished compared to DOPC than for Mastoparan-X. In general the association is weaker for mastoparan than for mastoparan-X. This is rather astonishing since an inspection of the amino-acid composition shows a slightly enlarged hydrophobicity for mastoparan. The charged amino-acids are identical and at the same position. The circular dichroism in solution indicates a slightly increased amount of  $\alpha$ -helical structure for mastoparan ( $\theta_0 = 7400 \text{ mdeg/dmol cm}$  in comparison to about

4000 mdeg/dmol cm in case of mastoparan-X), which might explain the finding. Experiments with melittin and DOPC vesicles also showed an increased binding with increasing salt concentration and a stronger binding for DOPC compared to POPC vesicles [13,22]. In contrast to our investigations, the isotherms for mastoparan and melittin were obtained by employing only circular dichroism. In all cases a slight time-dependence of the CD-signal within the first 5 min was observed, which might indicate a flip-flop process. In the fluorescence experiments no such behaviour was found.

However, a comparison of the different peptide–lipid systems on the basis of thermodynamic parameters by fitting a model based on partitioning of monomers to the data is not necessarily illuminating due to possible aggregation on the membrane as has been outlined in the simulations. Indeed, no definite correlation between salt concentration or vesicle size and the fit parameters could be found. Actually, in case of the peptide mastoparan-X, which is known to form pore structures, the existence of at least a small number of oligomers is quite probable. It was reported in [23] that under certain conditions (no added salt, pH 3, DMPC vesicles, labelled peptide) distinct tetrameric aggregates could be identified. Interpretation of observed changes in the fit parameters in dependence on experimental parameters seem to be difficult in general in such cases. Altogether we note that the overall appearance for the various lipid–peptide systems is the same, although the fitted parameters based on monomer partitioning depend in each case individually on the ionic-strength, lipid-composition and vesicle size.

Apart from this, one has to assume a far bigger error for the absolute values of the fit parameters than usually given even in absence of aggregation. Due to the numerical sensitivity (dependence on  $F_{\infty}$ , interdependence of the fit parameters, sensitivity on variations in the distribution of data points) the partition coefficient can vary by a factor of 0.5 to 2, the effective charge by about 0.8 to 1.2 for an identical experiment. In light of these error ranges, the fitted parameters are more or less identical.

Nevertheless, the averaged isotherms themselves are quite reliable so that one can determine the amount of bound peptide. One has to expect an error in the range of 10% for large  $r$  and of about 20% for

low  $r$  within the concentration range employed here. For the calculation of the amount of bound peptide in an extrapolation of the data to very low  $c_f$ , the error for  $r$  would be as large as for the partition coefficient.

## 6. Conclusions

1. It is shown that a pertinent correction for light scattering effects in measured circular dichroism or fluorescence signals must be applied in order to obtain reliable binding data.
2. Titration of several different peptide concentrations with liposomes are essential for the determination of a model-free association isotherm. There is, however, always some inevitable degree of uncertainty arising from the fact that vesicle preparations are not perfectly reproducible and titration errors not completely avoidable. However, the amount of bound peptide can be determined reasonably exact with the applied methods.
3. Anyway, the association isotherms can be sufficiently well fitted in terms of a monomer–monomer partitioning equilibrium described by a thermodynamic partition coefficient and effective charge number.
4. Aggregation of lipid associated peptide cannot generally be excluded so far as the observed curve fit is concerned. Therefore the fitted parameters do not necessarily represent well defined thermodynamic parameters.

## Acknowledgements

This work has been supported by grant no. 31.32188.91 from the Swiss Science Foundation.

## References

- [1] Y. Hirai, T. Yasuhara, H. Yoshida, T. Nakajima, M. Fujino, C. Kitada, *Chem. Pharm. Bull.* 27 (1979) 1942–1945.
- [2] Y. Hirai, M. Kuwada, T. Yasuhara, H. Yoshida, T. Nakajima, *Chem. Pharm. Bull.* 27 (1979) 1945–1946.
- [3] Y. Hirai, Y. Ueno, T. Yasuhara, H. Yoshida, T. Nakajima, *Biomedical Research* 1 (1980) 185–187.
- [4] A. Argiolas, J.J. Pisano, *Biol. Chem.* 258 (1983) 13697–13702.

- [5] T. Higashijima, S. Uzu, T. Nakajima, E.M. Ross, *J. Biol. Chem.* 263 (1988) 6491–6494.
- [6] M. Danilenko, P. Worland, B. Carlson, E.A. Sausville, Y. Sharoni, *Biochem. Biophys. Res. Commun.* 196 (1993) 1296–1302.
- [7] A. Arbuzova, G. Schwarz, *Progr. Colloid Polym. Sci.* 100 (1995) 345–350.
- [8] G. Schwarz, A. Arbuzova, *Biochim. Biophys. Acta* 1239 (1995) 51–57.
- [9] K. Wakamatsu, A. Okada, T. Miyazawa, M. Ohy, T. Higashijima, *Biochemistry* 31 (1992) 5654–5660.
- [10] K. Wakamatsu, T. Higashijima, M. Fujino, T. Nakajima, T. Miyazawa, *FEBS Lett.* 162 (1983) 123–126.
- [11] G. Schwarz, S. Stankowski, V. Rizzo, *Biochim. Biophys. Acta* 861 (1986) 141–151.
- [12] G. Schwarz, *Biophys. Chem.* 58 (1996) 67–73.
- [13] G. Schwarz, G. Beschiaschvili, *Biochim. Biophys. Acta* 979 (1989) 82–90.
- [14] S. Rex, *Biophys. Chem.* 58 (1996) 75–85.
- [15] C.F.J. Böttcher, C.M. van Gent, C. Fries, *Anal. Chim. Acta* 24 (1961) 203–204.
- [16] R.M. Peitzsch, M. Eisenberg, K.A. Sharp, S. McLaughlin, *Biophys. J.* 68 (1995) 729–738.
- [17] S. Stankowski, *Biophys. J.* 60 (1991) 341–351.
- [18] G. Schwarz, H. Gerke, V. Rizzo, S. Stankowski, *Biophys. J.* 52 (1987) 685–692.
- [19] G. Schwarz, U. Blochmann, *FEBS Lett.* 318 (1993) 172–176.
- [20] N. Hellmann, Ph.D. Thesis, University of Basel, Switzerland, 1995.
- [21] U. Blochmann, Ph.D. Thesis, University of Basel, Switzerland, 1992.
- [22] G. Beschiaschvili, Ph.D. Thesis, University of Basel, Switzerland, 1987.
- [23] K. Fujita, S. Kimura, Y. Imanishi, *Biochim. Biophys. Acta* 1195 (1994) 157–163.